Theory of friction: Stress domains, relaxation, and creep

B. N. J. Persson
Institut für Festkörperforschung, Forschungszentrum Jülich, D-52425 Jülich, Germany
(Received 3 November 1994; revised manuscript received 17 January 1995)

I discuss the microscopic nature of a block-substrate interface during sliding of an elastic block on a substrate with a lubrication film of molecular thickness (boundary lubrication). Arguments are given that the lubrication film at low sliding velocities has a granular structure, with pinned adsorbate domains accompanied by elastic stress domains in the block and substrate. At zero temperature, the stress domains form a "critical" state, with a continuous distribution $P(\sigma)$ of local surface stresses σ extending to the critical stress σ_a, necessary for fluidization of the pinned adsorbate structure. During sliding adsorbate domains will fluidize and refreeze. During the time period that an adsorbate domain remains in a fluidized state, the local elastic stresses built-up in the elastic bodies during "sticking" will be released, partly by emission of elastic wave pulses (sound waves) and partly by shearing the lubrication fluid. The role of temperature-activated processes (relaxation and creep) is studied and correlated with experimental observations. In particular, the model explains in a natural manner the logarithmic time dependence observed for various relaxation processes; this time dependence follows from the occurrence of a sharp steplike cutoff at $\sigma=\sigma_a$ in the distribution $P(\sigma)$ of surface stresses. Finally, I suggest a simple experiment to test directly the theoretical predictions: by registering the elastic wave pulses emitted from the sliding junction, e.g., by a piezoelectric transducer attached to the elastic block, it should be possible to prove whether, during uniform sliding at low velocities, rapid fluidization and refreezing of adsorbate domains occur at the interface.

I. INTRODUCTION

The study of sliding friction is one of the oldest problems in physics and certainly one of the most important from a practical point of view.[1,2] In spite of this, the microscopic origin of sliding friction is still not well understood.[3–6]

A common experimental observation is that the force necessary to slide a block on a substrate is nearly velocity independent at low sliding velocities. It was realized by Tomlinson[7] that this can be understood if, during sliding, rapid processes occur somewhere in the system even if the center of mass of the block moves *arbitrarily slowly* relative to the substrate. A fundamental problem in sliding friction is to understand the microscopic origin of these rapid processes, and to relate them to the macroscopic motion of the block.

Very recently, sliding friction measurements have been performed by Israelachvili and co-workers[8–10] and Granick and co-workers[11,12] using mica surfaces which can be produced atomically smooth (e.g., without a single step) over macroscopic areas. In these experiments a mica block is slid on a mica substrate with an intervening lubrication fluid. A spring is connected to the mica block and the free end of the spring is moved with a velocity v_s, which typically is kept constant but sometimes is allowed to change in time. The force in the spring is registered as a function of time and is the basic quantity measured in most of these friction studies. One remarkable result of these studies is that smooth sliding typically occurs even for spring velocities as low as $v_s \sim 1$ μm/s, while stick-and-slip motion is observed at lower spring velocities. Computer simulations[13–16] have shown, however, that a molecular thin fluid slab sheared between two solid surfaces is already unstable against freezing at high sliding velocities, say $v \sim 10$ m/s. Why, then, is smooth sliding observed at much lower sliding velocities?

One recent suggestion by Thompson and Robbins[13] is that the large mass of the block inhibits the freezing transition. Their argument is as follows: In order for the block to stop, its kinetic energy must be converted into potential energy in the film. The maximum potential energy that can be stored in the film is of the order of $\sim aF_0$ where a is a lattice constant of the block and F_0, the static friction force. Equating this with the kinetic energy at $v=v_c$ gives

$$v_c \sim (aF_0/M)^{1/2} ,$$

where M is the mass of the block. However, I have shown that this explanation for the occurrence of the critical speed v_c is incorrect, since the block as a whole will never stop abruptly, but initially only the bottom surface of the block stops and the inertia forces involved in this are negligible.[17] An elastic stopping wave will then propagate toward the upper surface of the block, and after the time period $\Delta t = d/c$ the whole block will be standing still, where c is the transverse sound velocity of the block and d the thickness of the block.

In a recent publication[17] I suggested that even if the motion of a macroscopic block is smooth for $v_s > v_c \sim 1$ μm/s, the lubrication layer is not in a smooth fluid state, but rather consists of pinned domains which fluidize and refreeze during sliding. In this paper I study some implications of this idea, and show how several experimental observations involving slow (thermally induced) relaxa-

tion can be naturally explained based on this picture. I also propose a simple experimental test of the theory.

II. EXPERIMENTAL BACKGROUND

In this section I review measurements which show that slow relaxation processes are of fundamental importance in sliding friction, and that they occur not only in practical sliding systems, but also in very well-defined model systems.

Following pioneering experiments by Rabinowicz[18] for metals on metals, slow relaxation processes have been studied in great detail by the rock-friction community[19] because of its importance for earthquakes. These studies, together with a very detailed sliding friction study by Heslot *et al.*[20] for paper on paper, find the following.

(a) The static friction coefficient f_s increases with the duration τ of stationary contact before sliding in a way which is well described by

$$f_s = a + b \ln(\tau/\tau_0) ,$$

where, if $\tau_0 = 1s$, $b/a \approx 0.0405$ in the study of Heslot *et al.* for paper and $b/a \approx 0.012$ in the study of Dieterich for quartz sandstone. Note that a depends on the reference time τ_0; changing to the reference time τ_1 gives

$$f_s = a' + b \ln(\tau/\tau_1) ,$$

where $a' = a + b \ln(\tau_1/\tau_0)$.

(b) At low pulling velocities (typically $v < 0.1$ μm/s) there is evidence of slow relaxation processes. It is not possible to speak of a truly motionless stick state, but stress-induced creep occurs.

Let me now briefly review some of the remarkable observations by Yoshizawa and Israelachvili[8] and Reiter *et al.*[21] These studies involve the sliding of a mica block on a mica substrate with a molecular thin lubrication layer. A spring (spring constant k_s) is attached to the mica block, and the free end of the spring is moved with a velocity v_s which may vary with time. The mica surfaces are atomically smooth, e.g., without a single step, and the thickness of the lubrication film can be varied by varying the load on the block.[22] The thickness of the lubrication film is known to within ± 1 Å by studying the optical fringes from the system.

Yoshizawa and Israelachvili[8] found that for spring velocities below a critical velocity v_c, stick-and-slip motion occurs. Now, if the motion of the spring is stopped at some time $t = 0$ and then started again (with the same velocity as before stop) after a time delay τ, the magnitude of the first spike is generally *higher* than in the steady sliding state. The longer the stopping period τ, the greater the magnitude of the first spike, which is referred to as the striction spike.

In measurements by Reiter *et al.*[21] the response of the sliding system to an oscillatory spring velocity $v_s \sim \sin(\omega t)$ was studied. This method probes the viscoelastic properties of the sliding junction. In Ref. 21 it was found that after a return to the pinned state at a time $t = 0$, from having been in the sliding state for $t < 0$, the elastic coefficient κ of the pinned state increased monotonically with increasing stopping time τ.

III. THEORY

A. Background

We consider the sliding of a block on a substrate with a molecular thick lubrication layer (boundary lubrication). Let (x,y,z) be a coordinate system with the (x,y) plane at the upper surface of the block and the $z = d$ plane at the interface between the block and the substrate. On the surface $z = d$ of the block acts the tangential surface stress $-\sigma(\mathbf{x},t)$. I first assume that no spatial fluctuations of $\sigma(\mathbf{x},t)$ occur beyond the dimension of a lubrication molecule, but later I will discuss the case when this assumption no longer holds. In a mean-field type of treatment I replace $\sigma(\mathbf{x},t)$ with $\sigma(t)$ obtained from the microscopic stress $\sigma(\mathbf{x},t)$ by averaging over (or integrating out) the rapid (in space and time) fluctuating part of the motion of the lubrication molecules. Later, when considering the adsorbate structure under conditions where it has a granular structure [pinned solid islands in a two-dimensional (2D) fluid], the spatial fluctuations in $\sigma(\mathbf{x},t)$ will be explicitly taken into account. If $-\sigma(t)$ is the stress exerted by the lubrication molecules on the bottom surface of the block, then, according to Newton's law of action and reaction, the block must exert the stress $\sigma(t)$ on the layer of lubrication molecules. This will in general lead to some drift motion of the lubrication layer. Note, however, that the velocity v of the bottom surface of the sliding block is not identical to the drift velocity of the adsorbate layer. For example, if the block and substrate are made from identical material, then the drift velocity of the adsorbate layer will be half of the velocity of the bottom surface of the block. This follows directly from the symmetry: In a reference frame where the substrate moves with the velocity $-v/2$ and the block with the velocity $v/2$, the drift velocity of the adsorbate layer must, by symmetry, vanish.

As a background for what follows I briefly discuss the nature of the relation $\sigma = f(v)$ between σ and v, based on numerical simulations and theoretical arguments.[14–16] The simulations considered a system of point particles, interacting via Lennard-Jones pair potentials and moving on a corrugated substrate. Owing to the adsorbate-substrate coupling, each adsorbate experiences a friction force $-m_a \eta \dot{\mathbf{r}}$, proportional to its velocity $\dot{\mathbf{r}}$, and a fluctuating force (arising from the irregular thermal motion of the substrate atoms) related to the friction η and to the substrate temperature T via the fluctuation-dissipation theorem. The drift velocity v was obtained by averaging over all the adsorbates and over time.

The relation $\sigma = f(v)$ can have two qualitatively different forms. If the adsorbate layer is in a two-dimensional (2D) fluid state, which is always the case in some parts of the (θ, T) (θ is the adsorbate coverage) phase diagram, then the $\sigma = f(v)$ relation has the form indicated in Fig. 1(a). In this case the drift velocity will be nonzero for arbitrarily small σ. This is, of course, exactly what one expects for a fluid: an arbitrary weak external force can shear a fluid. Furthermore, no hysteresis is observed, i.e., the relation between σ and v does not depend on whether σ decreases from a high value or

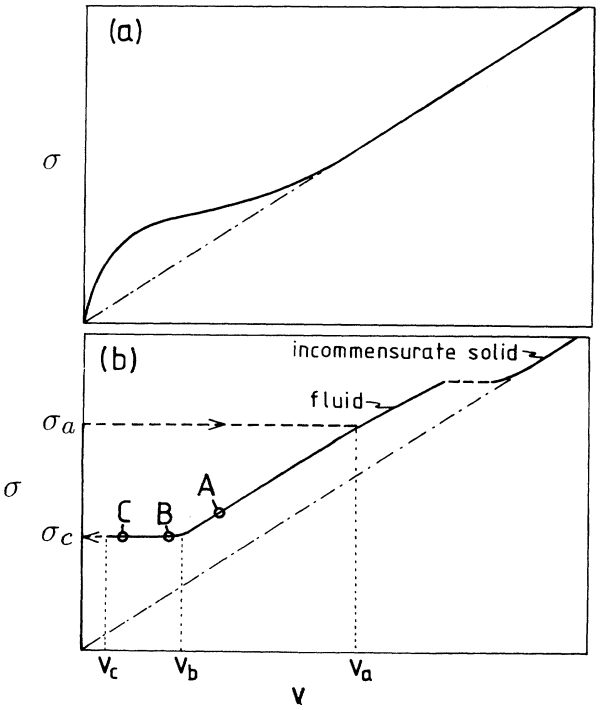

FIG. 1. The drift velocity $\langle v \rangle$ of an adsorbate layer as a function of the external stress σ. (a) The adsorbate layer is in a fluid state when $\sigma=0$. (b) The adsorbate layer is in a pinned solid state when $\sigma=0$. From Ref. 15.

increases from zero. Hence, if the lubrication layer in a sliding friction experiment is in a 2D fluid state, smooth sliding is expected (i.e., no stick-and-slip motion) for any spring velocity v_s. This is exactly what is observed experimentally. For example, Yoshizawa and Israelachvili[8] studied a 12-Å-thick hexadecane film between two smooth mica surfaces and found stick-and-slip motion when the temperature $T=17\,^{\circ}\mathrm{C}$, but smooth sliding for $T=25\,^{\circ}\mathrm{C}$. As will be shown below, stick-and-slip motion is observed when the adsorbate layer is in a pinned solid state at stick. Hence the melting temperature of the hexadecane film is somewhere between 17 and 25 °C.

Assume now instead that the system is in a part of the (θ,T) phase diagram where the adsorbate layer is in a solid state which is commensurate or at least pinned by the substrate. In this case the $\sigma=f(v)$ relation has the qualitative form shown in Fig. 1(b). If the system is first thermalized with $\sigma=0$ and then σ is increased, the pinned solid structure will remain, and the drift velocity is zero ($v=0$) until σ reaches some critical stress σ_a. At this point the adsorbate system fluidizes and the drift velocity increases abruptly from $v=0$ to v_a. If σ increases further, the drift velocity continues to increase as indicated in the figure. If σ is reduced below σ_a the system does not return to the pinned solid state at $\sigma=\sigma_a$ but continues to slide until σ reaches some lower critical stress σ_c, where the system abruptly returns to the pinned state.

The hysteresis shown in Fig. 1(b) can have two origins. The first follows from the fact that the temperature in the adsorbate systems during sliding is higher than that of the substrate, and might be so high that the fluid configuration rather than the solid pinned state is stable for $\sigma_c<\sigma<\sigma_a$. However, a more general explanation is the following. First, it has been found that the return to the pinned solid state is a nucleation process. However, a drag force will act on a pinned island, due to the surrounding flowing 2D fluid.[23] Assuming a circular pinned island, and that the drag force is uniformly distributed on the adsorbates in the island, the drag force is so large that the island will fluidize if $\sigma>\sigma_c=\sigma_a/2$.

Note that the $\sigma=f(v)$ relation has a wide almost horizontal region for $v_c<v<v_b$, where $\sigma\approx\sigma_c$. The lubrication layer in this sliding state is likely to consist of a granular fluid with pinned solid islands surrounded by 2D fluid. To see this, suppose we reduce the stress so that pinned islands start to occur. Now, if the islands are pinned by both of the sliding surfaces simultaneously, then, since it will take time for an island to grow and since the block and the substrate are in relative motion, during the growth of an island there will be a force on the island building up due to the local (at the island) elastic deformations of the block and substrate. If the force on the island becomes large enough, the island will fluidize. On the other hand, if an island is initially pinned by only one of the two sliding surfaces with different islands being pinned by either of the two different surfaces, then collisions between pinned islands would occur during the sliding process which would result in fluidization of islands. Both of these processes should result in a granular sliding state for the adsorbate layer, where pinned islands are continuously formed and fluidized. To what extent these effects are important in practice will depend on the

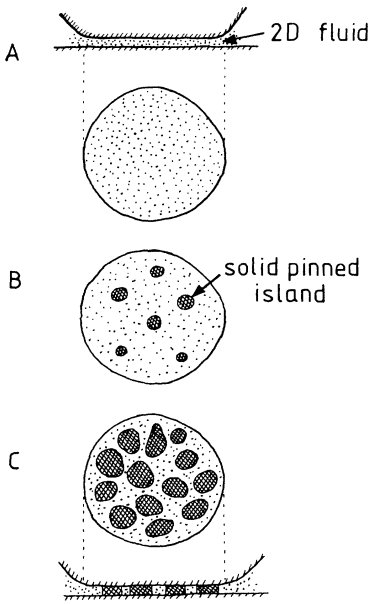

FIG. 2. Hypothetical structures of the adsorbate layer at points A, B, and C in Fig. 1 (schematically).

nucleation and growth rate of the pinned islands and on the sliding velocity v. At very low sliding velocity (creep) one expects the lubrication layer to consist almost entirely of pinned adsorbate domains and the associated stress domains in the block and the substrate. Figure 2 shows snapshot pictures of how the lubrication layer may look at points A, B, and C in Fig. 1(b).

The general form of the $\sigma = f(v)$ relation presented in Fig. 1(b) is supported by results of sliding friction measurements. Here I note only two facts: First, smooth sliding (i.e., sliding without stick and slip) is observed (if the damping is large enough that inertia effects can be neglected) in a large velocity interval $v_c < v_s < v_b$ where the friction force is almost velocity independent; this implies that the $\sigma = f(v)$ curve has a large almost horizontal region as indicated in Fig. 1(b). Second, direct support for a granular state with pinned regions and fluid regions comes from the study of Reiter *et al.*,[12] who probed the response of a sliding junction to an oscillatory external force. This study showed that although the dissipative stress in the sliding state was almost independent of sliding velocity (as long as it is not too large) significant (although smaller) elastic stress also persisted, which decreased with increasing deflection amplitude but was almost independent of oscillation frequency. The fact that elastic stresses occurred and that the elastic component decreased with increasing oscillation amplitude is a strong support for the existence of pinned islands; a larger oscillation amplitude would then imply stronger forces on the pinned islands and hence would tend to fluidize a larger fraction of them than would an oscillation of smaller amplitude; see Sec. III C.

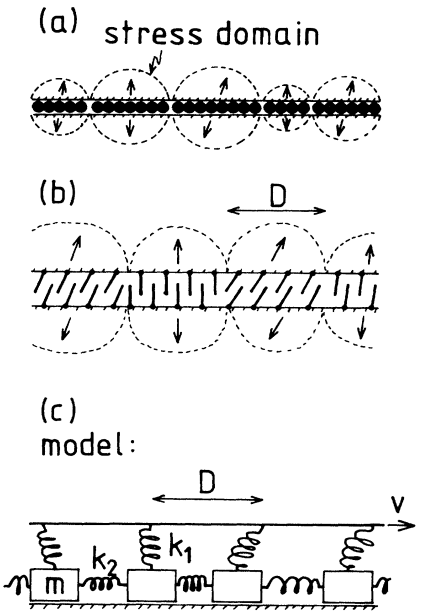

FIG. 3. (a) During sliding at very low velocity the adsorbate layer forms solid pinned domains. Associated with each domain is a stress field in the substrate and block. The arrows indicate the directions of thin cylindrical volume elements which would be perpendicular to the sliding surfaces when the stress fields vanish. (b) The same as (a) but for long-chain molecules (e.g., fatty acid molecules) bound to solid surfaces by one end. (c) A mechanical model used to describe the sliding properties of the interfaces in (a) and (b).

B. Stress domains and critical sliding state at zero temperature ($T = 0$ K)

The discussion above indicates that, at low sliding velocities, the lubrication film consists of solid domains which pins the relative position of the block and substrate. Associated with each adsorbate domain is a local stress domain in the elastic block and in the substrate; see Fig. 3(a). During sliding, the surface stress at a stress domain increases continuously until it reaches the critical value σ_a. At this point the adsorbate layer locally fluidizes, followed by a rapid local slip, during which the local stress in the block and substrate drops to a value close to zero. The elastic energy originally stored in the stress domain is partly radiated as elastic wave pulse into the block and substrate, and is partly consummated in shearing the lubrication fluid. After some short-time period the lubrication film refreezes and the whole process repeats itself.

I now present a simple model which captures the essential physics of the scenario outlined above. Assume that the width of a typical adsorbate domain (and accompanied stress domain) is D. The extent of the stress domain into the solid is of order $\sim D$. We replace the original system [Fig. 3(a)] with a model system [Fig. 3(c)] where each stress domain is replaced by a block (stress block) of mass $m = \rho D^3$, where ρ is the mass density of the original block. A stress block is connected to the main (or big) block by a spring k_1 and to the other nearby stress blocks with springs of magnitude k_2. The magnitudes of k_1 and k_2 can be estimated as follows. Let us first consider the block without the substrate. If a tangential surface stress of magnitude σ acts within the surface area $\delta A = D \times D$ it will induce a tangential displacement of δA by an amount $u \sim F/(\rho c^2 D)$, where $F = \sigma D^2$. This relation follows directly from elastic continuum theory; see Appendix B in Ref. 17. In the elastic continuum theory the elastic displacement field at distance D away from the center P of δA is about one third of the displacement of P. In the model system [Fig. 3(c)], if a force F acts on block 0, the resulting displacements q_i of the blocks can be determined by force equilibrium

$$k_1 q_i + k_2(2q_i - q_{i-1} - q_{i+1}) = F\delta_{i0} .$$

It is easy to calculate the displacements q_0 and $q_{\pm 1}$:

$$q_0 = \frac{F}{k_1 + 2k_2(1-\xi)} ,$$

$$q_{\pm 1}/q_0 = \xi ,$$

where

$$\xi = 1 + (k_1/k_2) - [2(k_1/k_2) + (k_1/k_2)^2]^{1/2} .$$

We now require that the displacement q_0 and the ratio $q_0/q_{\pm 1}$ agree with the elastic continuum model, where

these quantities equals $\sim F/(\rho c^2 D)$ and ~ 3, respectively. This gives $k_1 \sim k_2 \sim \rho c^2 D$. Now note the following: suppose first that the surface area δA is displaced by the distance u by an applied force F. At time $t=0$ the force F is abruptly removed. This result in an elastic wave pulse emitted into the elastic media, while u decays toward zero. We can include this damping mechanism in the model system [Fig. 3(c)] by introducing a damping force $-m\gamma(\dot{q}_i - \dot{x})$ in the equation of motion of the stress blocks ($\dot{x}$ is the velocity of the surface of the big block connecting the stress blocks to the big block). The damping γ can be estimated from the formula given in Ref. 24, $\gamma \sim k_1^2/(m\rho c^3)$. Using $k_1 \sim \rho c^2 D$ and $m \sim \rho D^3$, this gives $\gamma \sim c/D$. Note that this damping is of a magnitude similar to the resonance frequency $\omega_0 = (k_1/m)^{1/2} \sim c/D$. The strong damping is, of course, expected—any elastic displacement field set up at time $t=0$ within some volume $\sim D^3$ somewhere in the surface region of the big block and then set free will rapidly spread into the bulk of the big block: It has left the volume D^3 after the time period τ it takes for an elastic wave to propagate the distance D, i.e., $\tau \sim D/c$, so that the damping $\gamma \sim 1/\tau \sim c/D$. See also Ref. 25.

I have performed computer simulations based on the model shown in Fig. 3(c). I assume that the adsorbate domain related to stress block q_i is in a pinned solid state (so that $\dot{q}_i = 0$) until the elastic force

$$F = k_1(x - q_i) + k_2(q_{i+1} + q_{i-1} - 2q_i)$$

from the springs connected to block q_i reaches the critical force $F_a = \delta A \sigma_a$ necessary for fluidization of the pinned adsorbate structure. After fluidization the motion of q_i satisfies the Newton equation

$$m\ddot{q}_i = -m\gamma(\dot{q}_i - \dot{x}) - m_a\bar{\eta}\dot{q}_i + k_1(x - q_i) + k_2(q_{i+1} + q_{i-1} - 2q_i) \ . \quad (1)$$

The friction force $-m_a\bar{\eta}\dot{q}_i$ results from the drag force from the layer of adsorbed molecules. In the calculations below I assume that the adsorbate layer returns to the pinned state when $\dot{q}_i = 0$ at the end of the rapid local slip process. Alternatively, one may assume that the fluidized state exists for some average time τ before returning to the pinned solid state. Since the time it takes for the local surface stress to decay to zero at the fluidized island is very short (of order 10^{-10} s), it is very likely that at the return to the pinned state the local surface stress at the island is essentially zero. However, this condition is likely to give a very similar result to the condition that the return to the pinned state occurs when $\dot{q} = 0$, since with a physically reasonable damping γ the surface stress is quite small (on the scale of σ_a) when $\dot{q}$ reaches zero and the local motion stops.

In the application below we focus mainly on the creep region where $\dot{x}$ is very small and we can neglect this term in (1). Hence the damping term in (1) is $(m\gamma + m_a\bar{\eta})\dot{q}_i = m\bar{\gamma}\dot{q}_i$, which defines the effective damping coefficient $\bar{\gamma}$. From now on, I measure time in units of $(m/k_1)^{1/2}$, $\bar{\gamma}$ in units of $(k_1/m)^{1/2}$, distance in units of F_a/k_1, velocity in units of $F_a(mk_1)^{-1/2}$, force in units of F_a, and spring constants in units of k_1. In these units (1) becomes

$$\ddot{q}_i = -\bar{\gamma}\dot{q}_i + (x - q_i) + k_2(q_{i+1} + q_{i-1} - 2q_i) \ .$$

Note that from the estimates presented above $k_2 \sim 1$ and $\bar{\gamma} \sim 1$. I have solved the equation of motion (1) numerically by discretizing time in units $\Delta t = 0.005$. In all calculations presented in this paper I have chosen $\bar{\gamma} = 1$ and $k_2 = 1$. I have also performed calculations with other parameter values, but the qualitative picture is the same as that presented below. The model presented above is similar to a model studied by Burridge and Knopoff[26] and Carlson and Langer.[27] However, the friction law I use differs from theirs and the physical picture behind the models differs. The stress blocks in our model have a finite size determined by the diameter of a pinned adsorbate island, while Carlson and Langer were interested in the continuum limit where the size of a block vanishes. Furthermore, the main aim of this paper is to study the influence of thermal processes on the sliding and relaxation dynamics, and, as far as I know, this topic has not been studied before within the present model.

In Fig. 4(a) I show the friction force (per stress block)

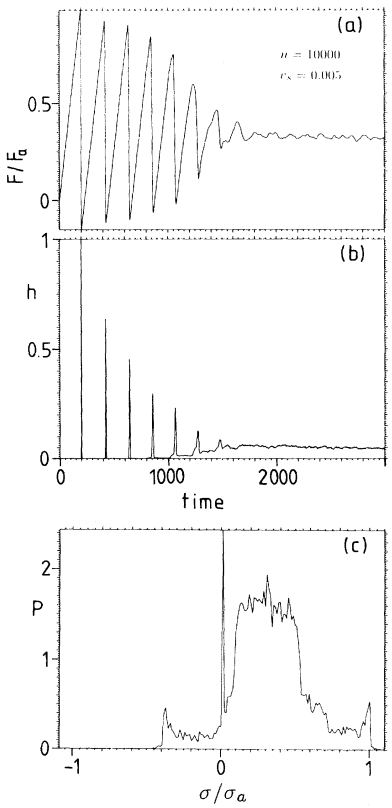

FIG. 4. (a) The friction force as a function of time. Initially the stress blocks are distributed very regularly on the surface, and many stick-and-slip periods occur before the system reaches a steady state. (b) The function $h(t)$ is the fraction of the blocks which are moving at time t. (c) The distribution of surface stresses in the steady state. In the calculation $k_1 = k_2 = \bar{\gamma} = 1$, $v_s = 0.005$ and $n = 10\,000$ stress blocks.

as a function of time when the sliding velocity $v_s = 0.005$. In the calculation I used $n = 10\,000$ stress blocks which initially ($t = 0$) were distributed very regularly on the surface (the initial coordinates was taken as $q_i = 0.01 \times r_i$, where r_i is a random number between 0 and 1) and many stick-and-slip periods occur before the system reaches a steady state. The function $h(t)$ shown in Fig. 4(b) is the fraction of the blocks which move at time t. Note that during the first slip period all stress blocks move (i.e., $h = 1$), while during the second slip period only $\sim 70\%$ of the blocks moves. The first few slip periods are separated by time intervals where no blocks move. However, for $t > 1000$ some blocks always move and, in particular, when the steady state has been reached ($t > 1800$) about $\sim 10\%$ of the blocks move at any time. This does not, of course, mean that the same blocks are moving the whole time, but that each individual block performs a stick-and-slip type of motion, and that avalanches of varying sizes occur (see Sec. III D) in such a manner that about 10% of the blocks move at any given time. Finally, Fig. 4(c) shows the distribution of surface stresses in the steady state. Note that the distribution $P(\sigma)$ is critical, i.e., that a continuous distribution of local surface stresses σ occurs, which *extend to the critical stress* σ_a, *necessary for fluidization of the pinned adsorbate structure.* This implies that thermal processes will be very important at low sliding velocities (see Sec. III C). Note that the surface stress σ is negative for about 5% of the blocks; this effect results from inertia and corresponds to stress blocks which during sliding picked up enough kinetic energy to overshoot, so that when returning to the stick state the sum of the spring forces acting on such a block is negative. The sharp peak close to $\sigma = 0$ in Fig. 4(c) corresponds to a small fraction of blocks which slide with a velocity close to the driving velocity $v_s = 0.005$ so that a kinetic friction force of magnitude $\bar{\eta}\dot{q} \sim 0.005$ acts on these blocks. In contrast, most of the blocks perform a very rapid motion during slip, where velocities of order 1 occur. At sliding velocities lower than 0.005, the sharp peak in Fig. 4(c) disappears and the distribution $P(\sigma)$ converges towards velocity-independent distribution which looks virtually identical to the one in Fig. 4(c); i.e., $v_s = 0.005$ is small enough to be practically in the asymptotic small-v_s regime. This velocity region will be our main concern below.

Figure 5 shows the same quantities as in Fig. 4 but for a higher sliding velocity $v_s = 0.03$. Note the sharp peak in Fig. 5(c) which carries about 50% of the blocks, i.e., about half of the blocks, now performs a slow drift motion $\dot{q} \sim v_s$ where the surface stress equals $\sigma \sim \bar{\eta} v_s = 0.03$. However, some of the blocks still perform rapid slip motion, giving rise to the broad distribution in $P(\sigma)$ extending from $\sigma = -0.4\sigma_a$ to σ_a. For sliding velocities above $v_s = 0.05$ all stress blocks slide with the speed v_s, and the stress distribution $P(\sigma)$ equals a Dirac δ function centered at $\sigma_s = \bar{\eta} v_s$.

The dashed lines in Figs. 6(a) and 6(b) show, in the steady-state sliding regime, the dependence of the friction force and the fraction of sliding blocks on the natural logarithm of the sliding velocity. These curves have been

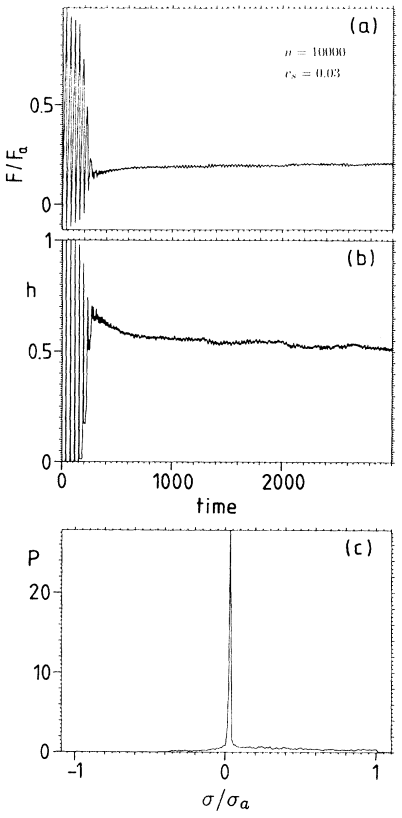

FIG. 5. The same as Fig. 4, but with $v_s = 0.03$.

constructed from many computer simulations of the type shown in Figs. 4 and 5. Note the following: (a) For $\ln(v_s) \leq -5$, i.e., $v_s < 0.006$, the friction force is velocity independent. As discussed above, in this velocity region the stress distribution $P(\sigma)$ is velocity independent and the number of stress blocks moving at any given time is proportional to the sliding velocity (not shown). Hence, a velocity-independent sliding friction force is indeed expected. For $\ln v_s \geq -3$ or $v_s > 0.05$ all stress blocks move with velocity v_s and the friction force is given by $\bar{\eta} v_s$. As a function of $\ln(v_s)$ this gives the rapidly increasing friction force shown in Fig. 6(a) for $\ln(v_s) \geq -3$. In this case $P(\sigma)$ is a Dirac δ function centered at $\bar{\gamma} v_s$. Finally, in the transit region $-5 < \ln(v_s) < -3$, the friction force varies smoothly from its small-v_s asymptotic value to the high velocity behavior where all blocks slide with the velocity v_s. In this transit region $P(\omega)$ has both a broad continuum extending from $\sim -0.4\sigma_a$ to σ_a as well as a Dirac δ-function contribution centered at a stress close to the frictional stress experienced by a block which slides at the speed v_s.

C. Relaxation and creep ($T > 0$ K)

The calculations presented in Sec. III B were for zero temperature, where no thermal excitations can occur. We have seen that during sliding at low velocity v the dis-

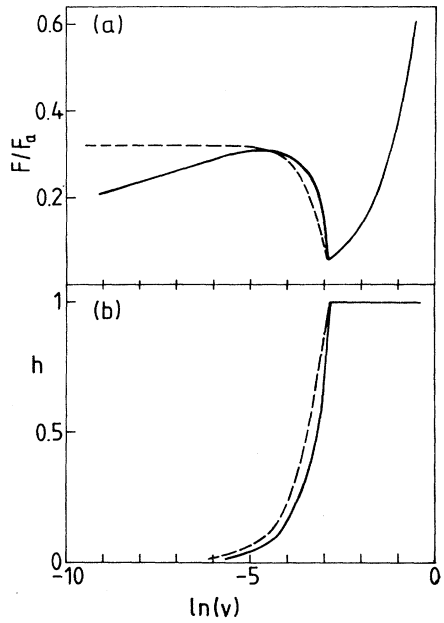

FIG. 6. (a) The friction force in the steady state as a function of the natural logarithm of the sliding velocity. (b) The fraction of sliding blocks as a function of the natural logarithm of the sliding velocity. The solid lines include thermally activated processes ($\nu=0.1$ and $\beta=40$), while the dashed lines are for zero temperature.

tribution $P(\sigma)$ is critical, i.e., the distribution $P(\sigma)$ of local surface stresses has a sharp steplike cutoff at $\sigma=\sigma_a$; see Fig. 4(c). This implies that thermally activated processes will be very important at low sliding velocities, since those stress blocks which have surface stresses in the vicinity of $\sigma=\sigma_a$ may be thermally exited over the small elastic energy barrier which separate them from the sliding state. In fact, if v is small enough this channel of going over the barrier will occur before a stress block would be driven over the barrier by the motion $x=x(t)$. Similarly, thermal processes are crucial during stop: if no thermal excitations occur (i.e., zero temperature) the distribution $P(\sigma)$ at stop would be time independent and of the form shown in Fig. 4(c) with some stress blocks with σ just below σ_a. At nonzero temperature, an arbitrary small thermal fluctuation can kick these blocks over the barrier to the sliding state. In this section I introduce thermal excitations in a realistic manner and study their influence on the sliding dynamics.

We assume that during sliding a stress block satisfies the same equation of motion (1) as in Sec. III B. This is certainly a good approximation, since during local sliding large velocities occurs and small thermal fluctuations should be of no importance. Now consider a pinned stress block. In Sec. III B it was assumed that the block remains pinned until the force on the block from the springs connected to it reaches the critical value F_a. At this point the adsorbate layer fluidizes and local slip motion occurs. I now generalize this assumption in order to allow the stress blocks to be thermally excited over the barrier toward motion. Let us consider a stress block i with a coordinate q_i. The potential energy stored in the springs connected to this block is

$$U=\tfrac{1}{2}k_1(x-q_i)^2+\tfrac{1}{2}k_2(q_{i+1}-q_i)^2+\tfrac{1}{2}k_2(q_{i-1}-q_i)^2 , \quad (2)$$

and the force on block i is

$$F=k_1(x-q_i)+k_2(q_{i+1}+q_{i-1}-2q_i) ,$$

which must be below F_a in order for the block to be pinned. Now, considered $U=U(q_i)$ as a function of q_i (i.e., $q_{i\pm1}$ fixed). $U(q_i)$ has the form indicated in Fig. 7. If we define the critical displacement q_i^0 by

$$F_a=k_1(x-q_i^0)+k_2(q_{i+1}+q_{i-1}-2q_i^0) ,$$

i.e.,

$$q_i^0=\frac{k_1x+k_2(q_{i+1}+q_{i-1})-F_a}{k_1+2k_2} . \quad (3)$$

Then the elastic barrier $\Delta E=U(q_i^0)-U(q_i)$ must be overcome by thermal excitation in order to initiate sliding; see Fig. 7. According to statistical mechanics, the probability rate w for thermal excitation over a barrier of height ΔE can be written (see Appendix A)

$$w=\nu e^{-\beta\Delta E} .$$

When studying the time evolution of the system, time is discretized in steps of length Δt. The probability that the stress block jumps over the barrier during the time Δt is $w\Delta t$. Since the actual excitation over the barrier occurs in a stochastic manner as a function of time, we use random numbers to determine when the jump occurs. That is, if r is a random number between 0 and 1 then if $r<w\Delta t$ the jump is assumed to have occurred during the time period Δt while the stress block remains in the pinned state if $r>w\Delta t$. In all calculations below I have

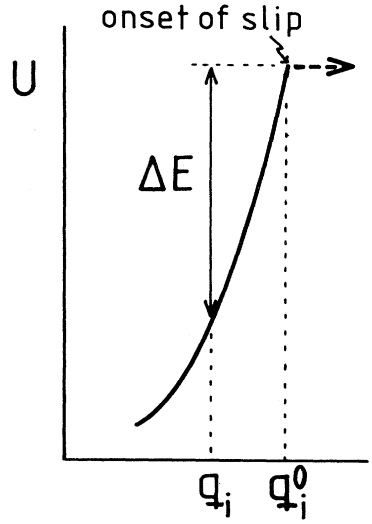

FIG. 7. The elastic potential energy as a function of the coordinate q_i of block i ($q_{i\pm1}$ are fixed). At the critical displacement the $q_i=q_i^0$ slip starts.

used $\nu=0.1$ and $\beta=40$. I have also performed calculations for other parameter values, but the same qualitative picture results.

Figure 8 is obtained with the same model parameters as in Fig. 4 except that thermal excitation is included as discussed above. Note that when thermal excitation is included, the onset of the first slip occurs at a lower static friction force; $F_{\max}$ is reduced from $0.98F_a$ in Fig. 4(a) to $0.70F_a$ in Fig. 8(a). Furthermore, the number of stick-and-slip oscillations before the steady-state sliding regime is reached is reduced. Even more dramatic is the change in the fraction of blocks which moves at time t, compare Figs. 4(b) and 8(b). While without thermal excitation all the stress blocks move during the first slip period, only $\sim 30\%$ move when thermal excitation is included. The stress distribution $P(\sigma)$ in the steady-state region [see Fig. 8(c)] is qualitatively similar to that without relaxation [see Fig. 4(c)].

The solid line in Fig. 6(a) shows the friction force in the steady-state sliding regime, as a function of the natural logarithm of the sliding velocity, as obtained from many computer simulations of the type shown in Fig. 8. This result differs most importantly from the zero-temperature results (dashed line) by the linear increase of the friction force with increasing $\ln(v)$, $F/F_a=0.44+0.026\ln(v)$ for $\ln(v)\leq -5.5$. Note that in this velocity region, when thermal excitation is taken into account, a smaller external force generates the same sliding velocity as a larger force in the absence of thermal processes. This creep motion results from thermal excitation of stress blocks from close to $\sigma=\sigma_a$, over the barrier to the sliding state. Hence a given block does not need to be pulled over the barrier by the motion v, but can jump over the barrier by thermal excitation. Figure 6(b) shows the fraction of sliding blocks as a function of the natural logarithm of the sliding velocity. The solid line includes thermal processes, while the dashed lines are the zero-temperature result.

Figure 9 illustrates the slow relaxation which occurs if the sliding velocity is abruptly reduced from a nonzero value to zero. The time variation of the friction force is shown in Fig. 9(a), and that of the fraction of moving blocks in Fig. 9(b). For $t<1000$ the sliding velocity $v_s=0.005$. At $t=1000$ the sliding velocity is set equal to zero ($v_s=0$). The decay of F and h with increasing time for $t>1000$ is due to thermal excitation (relaxation). Figure 10(a) shows the friction force [from Fig. 9(a)] during the relaxation-time period, as a function of the natural logarithm of the stopping time $\tau=t-1000$. Note that except for very short and very long times, F decays proportional to the logarithm of the stopping time τ; the dashed line is given by $F(\tau)/F_a=0.38-0.044\ln(\tau)$. Finally, Fig. 10(b) shows the stress distribution at the end of the relaxation process in Fig. 12(a), i.e., for $t=3000$. Note that the distribution is no longer critical; i.e., all the stress blocks which occurred close to $\sigma=\sigma_a$ have been removed by thermal excitation. As $\tau\rightarrow\infty$ the distribution $P(\sigma)$ narrows and $F\rightarrow 0$, but it is not possible to ob-

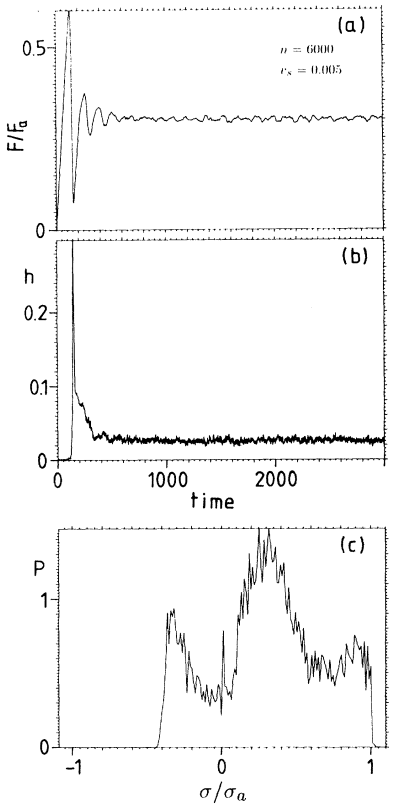

FIG. 8. The same as Fig. 4, except that thermally activated processes are included as discussed in the text. $\nu=0.1$ and $\beta=40$.

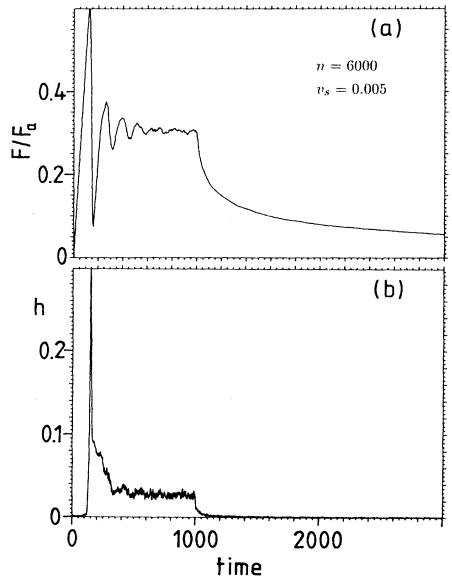

FIG. 9. The time variation of (a) the friction force and (b) the fraction of moving blocks. For $t<1000$ the sliding velocity $v_s=0.005$. At $t=1000$ the sliding velocity is set equal to zero ($v_s=0$), and the observed time variations of F and h for $t>1000$ are due to thermally excited processes (relaxation). In the calculation, $\nu=0.1$ and $\beta=40$.

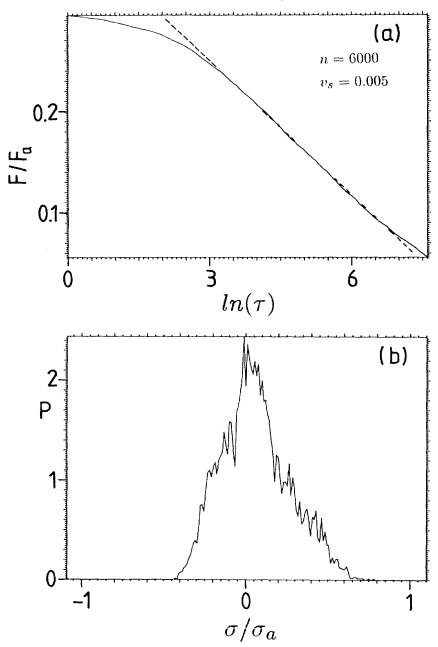

FIG. 10. (a) The friction force [from Fig. 9(a)] during the relaxation-time period, as a function of the natural logarithm of the stopping time $\tau = t - 1000$. The dashed line is given by $F(\tau)/F_a = 0.38 - 0.044 \ln(v)$. (b) The stress distribution at the end of the relaxation process in Fig. 9(a), i.e., for $t = 3000$. $\nu = 0.1$ and $\beta = 40$.

tain this fully relaxed state in a computer simulation because of the long stopping time τ necessary.

Figure 11 shows another manifestation of relaxation in a computer simulation of stop and start. For $t < 600$ the sliding velocity $v_s = 0.01$. For $600 < t < 2600$ the sliding velocity vanishes ($v_s = 0$). For $t > 2600$ the sliding velocity $v_s = 0.01$. In Fig. 11(a) the friction force is shown as a function of time. Note the striction spike of height ΔF. The fraction of blocks moving at time t is shown in Fig. 11(b). The stress distribution at the end of the sliding process ($t = 3000$) is shown in Fig. 11(c). The circles in Fig. 12 show the height ΔF of the striction spikes as a function of the stopping time τ from several computer experiments of the type shown in Fig. 11. The solid line is determined by $\Delta F/F_a = -0.19 + 0.05 \ln(\tau)$.

It is possible, with a simple model calculation, to understand why the relaxation processes studied above have the asymptotic time dependences $\sim \ln(\tau)$ and why the creep motion depends on velocity as $\sim \ln(v)$. Let us first consider how the force acting on the big block decreases with time after the sliding motion has abruptly been stopped at time $t = 0$ [see Fig. 9(a)]. I will use a mean-field-type approximation in estimating the elastic barrier ΔE which a pinned stress block must overcome by thermal excitation before sliding. The exact elastic barrier for block i in Fig. 3(c) was calculated in Sec. III B, and depends on the positions of blocks $i \pm 1$:

$$\Delta E = U(q_i^0) - U(q_i) \ .$$

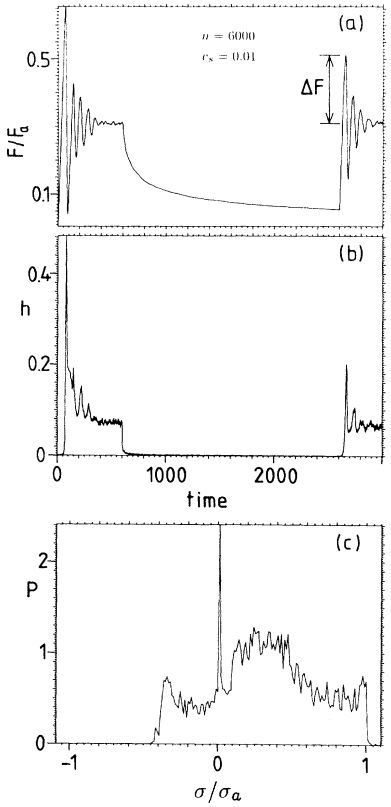

FIG. 11. A computer simulation of stop and start. For $t < 600$ the sliding velocity $v_s = 0.01$. For $600 < t < 2600$ the sliding velocity vanishes ($v_s = 0$). For $t > 2600$ the sliding velocity $v_s = 0.01$. (a) The friction force as a function of time. Note the striction spike of height ΔF. (b) The fraction of blocks moving at time t. (c) The stress distribution at the end of the sliding process ($t = 3000$).

In the expression for U we replace $q_{i\pm1}$ by their average values q. Using (2) and (3) this gives

$$\Delta E = \frac{F_a^2 - F^2}{2(k_1 + 2k_2)} \ ,$$

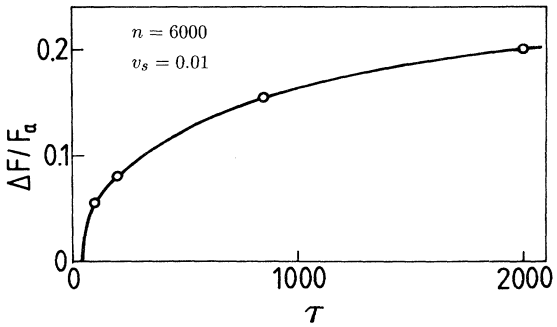

FIG. 12. Circles represent the height ΔF of the striction spikes as a function of the stopping time τ from computer experiments of the type shown in Fig. 11. The solid line is determined by $\Delta F = -0.19 + 0.05 \ln(\tau)$.

where $F=k_1(x-q_i)+2k_2(q-q_i)$ is the mean-field force acting on block i. In terms of the surface stress $\sigma=F/\delta A$, we have

$$\Delta E=\epsilon[1-(\sigma/\sigma_a)^2] , \tag{4}$$

where

$$\epsilon=\frac{(\delta A\sigma_a)^2}{2(k_1+2k_2)}=\frac{F_a^2}{2(k_1+2k_2)} . \tag{5}$$

Assume that no slip has occurred at time $t=0$. The probability that the block has not jumped over the barrier ΔE at time $t>0$ is

$$P(t)=e^{-wt} , \tag{6}$$

where the rate coefficient w has the form

$$w=\nu e^{-\beta\Delta E} , \tag{7}$$

where ν is a prefactor and $1/\beta=k_BT$. Now, assume that at the interface between the big block and the substrate occur $N_0\gg1$ stress blocks. The total number of stress blocks which, at time $t>0$, remain in their original ($t=0$) positions, is given by

$$N(t)=\sum_i P_i(t)=\sum_i e^{-w_it} . \tag{8}$$

Let $P(\sigma)$ be the distribution of surface stresses at time $t=0$. Let us first assume that $P(\sigma)$ is uniform, i.e., that $P(\sigma)=1/\sigma_a$ for $0<\sigma<\sigma_a$ and zero otherwise. The actual distribution may not be uniform but the only relevant result for the present study is that there is a sharp steplike cutoff in the distribution $P(\sigma)$ at $\sigma=\sigma_a$. In this case, using (4) and (6)–(8), we obtain

$$N(t)=N_0\int_0^{\sigma_a}d\sigma\,P(\sigma)e^{-\nu t\exp\{-\beta\epsilon[1-(\sigma/\sigma_a)^2]\}} , \tag{9}$$

where $N_0=N(0)$ is the total number of stress blocks. If we introduce $\sigma=\sigma_a(1-\xi)$, and approximate

$$\sigma_a^2-\sigma^2\approx2\sigma_a^2\xi ,$$

and assume $P(\sigma)=1/\sigma_a$, from (9) we obtain

$$N(t)\sim N_0\int_0^1 d\xi\, e^{-\nu t\exp(-\beta2\epsilon\xi)} .$$

If we set

$$\eta=e^{-\beta2\epsilon\xi} ,$$

then

$$N(t)\sim\frac{N_0}{\beta2\epsilon}\int_{e^{-\beta2\epsilon}}^1\frac{d\eta}{\eta}e^{-\nu t\eta} . \tag{10}$$

Now, if $\beta\epsilon\gg1$ and $\nu t\gg1$, we can accurately approximate (10) with

$$N(t)\sim\frac{N_0}{\beta2\epsilon}\int_{e^{-\beta2\epsilon}}^{1/\nu t}\frac{d\eta}{\eta}=N_0\left[1-\frac{\ln(\nu t)}{\beta2\epsilon}\right] . \tag{11}$$

The asymptotic result $N_0-N(t)=\Delta N(t)\sim\ln(\nu t)$ is valid whenever the probability distribution $P(\sigma)$ has a steplike cutoff. On the other hand, if $P(\sigma)$ goes continuously to zero at $\sigma=\sigma_a$, then this asymptotic time dependence no longer holds. For example, if

$$P(\sigma)\sim(\sigma_a-\sigma)^n$$

as $\sigma\to\sigma_a$ from below, while $P=0$ for $\sigma>\sigma_a$, then it is easy to show that

$$\Delta N\sim[\ln(\nu t)]^n .$$

In particular, if $P(\sigma)$ has the triangular form $P=2(\sigma_a-\sigma)/\sigma_a^2$ if $0<\sigma<\sigma_a$, and zero otherwise, one obtains

$$\Delta N(t)/N_0=[\ln(\nu t)]^2/(\beta2\epsilon)^2 .$$

Formula (11) explains the $\ln(t)$ dependence found in the simulations above, and is in good quantitative agreement with the simulations. For example, consider the results in Fig. 9(a) for $F(t)/F_0$. To apply (11) to this case, let us note that when a stress block jumps over the elastic barrier, the force on the big block changes by roughly $\sigma_a\delta A$. Hence $F(0)-F(t)\approx\delta A\sigma_a\Delta N(t)$, and since $F_0=N_0\delta A\sigma_a$ we obtain $[F(0)-F(t)]/F_0\approx\Delta N/N_0$ or, using (11),

$$\frac{F(t)}{F_0}\approx\frac{F_k}{F_0}-\frac{1}{\beta2\epsilon}\ln(\nu t) , \tag{12}$$

where $F(0)=F_k=F_0/2$ is the kinetic friction force in the present model. Let us compare the mean-field results (12) with the results in Fig. 9(a). The dashed line in Fig. 10(a) is given by

$$F/F_0=0.38-0.044\ln(t) ,$$

which we can write as $F(t)/F_0=F_k/F_0-B\ln(bt)$, where $F_k/F_0=0.3$, $B=0.044$, and $b=0.15$. In the simulations $\beta=40$, and since $\epsilon=\frac{1}{6}$ the values for B and b in the mean-field model equal $1/2\beta\epsilon=0.075$ and $b=\nu=0.1$, in remarkably good agreement with the results of the simulation.

The analysis presented above assumed that the motion of the block is abruptly stopped at time $t=0$, i.e., $x(t)=\text{const}$ for $t>0$. More complex sliding and relaxation problems can be studied based on an equation of motion for the distribution function $P(\sigma,t)$. In Appendix B it is shown that

$$\frac{\partial P}{\partial t}=-\frac{k_1v}{\delta A}\frac{\partial P}{\partial\sigma}-\nu Pe^{-\beta\Delta E(\sigma)}+\delta(\sigma)\left[\int d\sigma'\nu P(\sigma',t)e^{-\beta\Delta E(\sigma')}+\frac{k_1v}{\delta A}P(\sigma_a,t)\right] . \tag{13}$$

The first term on the right-hand side of this equation describes the rate of change of $P(\sigma,t)$ due to the motion of the big block [velocity $v=\dot{x}(t)$]. The second term describes the probability rate for a stress block to be thermally excited over the barrier $\Delta E(\sigma)=U(\sigma_a)-U(\sigma)$. Finally, the last term, which is nonzero only if $\sigma=0$, describes the increase in the number of stress blocks with zero surface stress which results from all the stress blocks which have been thermally excited over the barrier $\Delta E(\sigma)=U(\sigma_a)-U(\sigma)$ or driven over the barrier by the motion $x(t)$; we assume that after fluidization of the adsorbate layer a block rapidly relaxes down to the state where the surface stress equals zero, after which the adsorbate layer refreezes and the block returns to the pinned state.

Note that (13) conserves probability: integrating (13) over σ from $-\sigma_a$ to σ_a and using $P(-\sigma_a,t)=0$ (we assume sliding along the positive x direction) gives

$$\frac{d}{dt}\int_{-\sigma_a}^{\sigma_a} d\sigma\, P(\sigma,t)=0 .$$

Hence, if the normalization condition

$$\int_{-\sigma_a}^{\sigma_a} d\sigma\, P(\sigma,0)=1 \tag{14}$$

is satisfied at time $t=0$, it will be automatically satisfied for all other times.

Let us study steady sliding. In this case $\partial P/\partial t=0$ and (13) reduces to an ordinary differential equation for $P(\sigma,t)\equiv P(\sigma)$, with the solution (see Appendix B)

$$P(\sigma)=Ce^{-(\delta A\nu/k_1 v)\int_0^{\sigma} d\sigma' \exp[-\beta\Delta E(\sigma')]} \tag{15}$$

if $0\le\sigma\le\sigma_a$, and zero otherwise. C is determined by the normalization condition (14). The force F which gives rise to the sliding velocity v is determined by the equation

$$F=\frac{\int_{-\sigma_a}^{\sigma_a} d\sigma\, A\sigma P(\sigma)}{\int_{-\sigma_a}^{\sigma_a} d\sigma\, P(\sigma)} . \tag{16}$$

Let us first consider the large-v limit. Assume that $\alpha\ll 1$ where $\alpha=F_a\nu/(2k_1 v\beta\epsilon)$. In this case, (15) and (16), to leading order in $\alpha\sim 1/v$ (see Appendix B), give

$$\frac{F}{F_0}\sim\frac{1}{2}-\frac{\alpha}{4\beta\epsilon}=\frac{1}{2}-\frac{F_a\nu}{2k_1 v}\left[\frac{k_B T}{2\epsilon}\right]^2 .$$

Next, let us consider sliding at small velocities, which we will refer to as creep motion. Assume that $\alpha\gg 1$ but $\alpha\exp(-2\beta\epsilon)\ll 1$. In this case (15) and (16) give (see Appendix B)

$$\frac{F}{F_0}\sim\frac{1}{2}+\frac{1}{4\beta\epsilon}\ln\left[\frac{2\beta\epsilon k_1 v}{F_a\nu}\right]=\frac{F_k}{F_0}+\frac{1}{4\beta\epsilon}\ln\left[\frac{2\beta\epsilon k_1 v}{F_a\nu}\right] . \tag{17}$$

Let us compare the prediction of this formula with Fig. 6. In the creep region, $\ln(v)\le -5$ in Fig. 6, F varies linearly with $\ln(v)$ in accordance with (17). The creep region in Fig. 6 is well described by

$$F/F_0=0.44+0.026\ln(v) ,$$

which we can write as $F/F_0=F_k/F_0+B\ln(bv)$, where $F_k/F_0=0.32$, $B=0.026$, and $b=118$. The corresponding values for B and b in our mean-field model [Eq. (17)] are 0.037 and 133, in remarkably good agreement with the simulations.

Finally, in the extreme low-v limit, where $\alpha\exp(-2\beta\epsilon)\gg 1$, Eqs. (15) and (16) give (see Appendix B)

$$F\sim(F_0/2\alpha\beta\epsilon)e^{\beta\epsilon}=N_0(k_1 v/\nu)e^{\beta\epsilon} . \tag{18}$$

Note that $F\ll F_0$, and that the friction force is proportional to the sliding velocity v. Formula (18) is of very limited practical use, however, since extremely low sliding velocities v are necessary for (18) to be valid.

Let me, in the light of the model results obtained above, discuss the experiments of Reiter *et al.*[21] They studied the elastic (and dissipative) behavior of a confined lubricant layer using oscillatory shear. The lubrication fluid (a 7±2 Å-thick layer of 3-methy-undecane, an alkane 11 CH_2 units long with one methyl side group) was localized between two atomically smooth mica crystals. The shear amplitude (i.e., the relative interfacial displacement amplitude) d was measured as a function of the amplitude of the applied oscillatory shear stress. Furthermore, the elastic stiffness κ (the ratio between the in-phase component of the responding stress and the deflection amplitude) was measured as a function of d. Measurements were performed at two different oscillation frequencies, 1 and 100 Hz, but the results were almost identical.

For a small enough applied shear force the lubrication layer behaved as an elastic solid and $\kappa=$const. However, as the onset of sliding was approached, the stiffness κ decreased and extrapolated to zero at a certain value $d=d_c$. This results can be easily understood based on the assumption that the lubrication layer in the pinned state consists of solid adsorbate domains and associated stress domains where the distribution of tangential surface stresses extend up to the stress σ_a necessary to fluidize a solid adsorbate layer. In this model, an external applied oscillatory stress will, roughly speaking, fluidize all adsorbate domains where the surface stresses occur in the interval $\sigma_a-\sigma_1<\sigma<\sigma_a$, where σ_1 is the amplitude of the oscillatory stress (induced by the external stress) which acts on a pinned solid adsorbate domain. Note that σ_1 is a function of d, $\sigma_1=\sigma_1(d)$. Now if, as a result of the oscillatory external shear stress, a fluidized adsorbate domain does not refreeze, then one expects κ to decrease monotonically as the shear amplitude d increases, until d reaches some critical value d_c where all solid adsorbate domains have fluidized [note that $\sigma_1(d_c)=\sigma_a$]. It is interesting to note that for d below a few Å, $\kappa=$const, i.e., is independent of d. But this is exactly what is expected from the model presented above when thermal processes are taken into account, since the stress blocks which would occur close to $\sigma=\sigma_a$ if no thermal excitations occur have jumped over the barriers and occur at $\sigma\approx 0$. Hence, roughly speaking, no stress blocks

occur for $\sigma_a - \Delta\sigma < \sigma < \sigma_a$ (where $\Delta\sigma$ increases with the time of contact prior to probing κ), and κ will remain constant as long as $\sigma_1(d) < \Delta\sigma$.

D. Discussion

What type of local slip events occur during sliding at low velocities? The fact that, in the steady state, the function $h(t)$ is very smooth (i.e., very weak noise) in Figs. 4 and 8, implies that the largest slip events (avalanches) must be very small compared with the total number of blocks used in the simulations (10 000 and 6000, respectively). To study the distribution of sizes of slip events, I consider a system consisting of only $n = 100$ blocks and a very low sliding velocity $v_s = 0.0002$. In this case the individual slip events can be resolved in time.

Figures 13(a) and 13(b) show the time variation of the friction force and of the fraction of moving blocks at zero temperature. Note that at a given time at most two blocks are sliding. However, most of the time no block or one block is sliding. In fact, when two blocks slide these are not necessarily two nearby blocks but could be

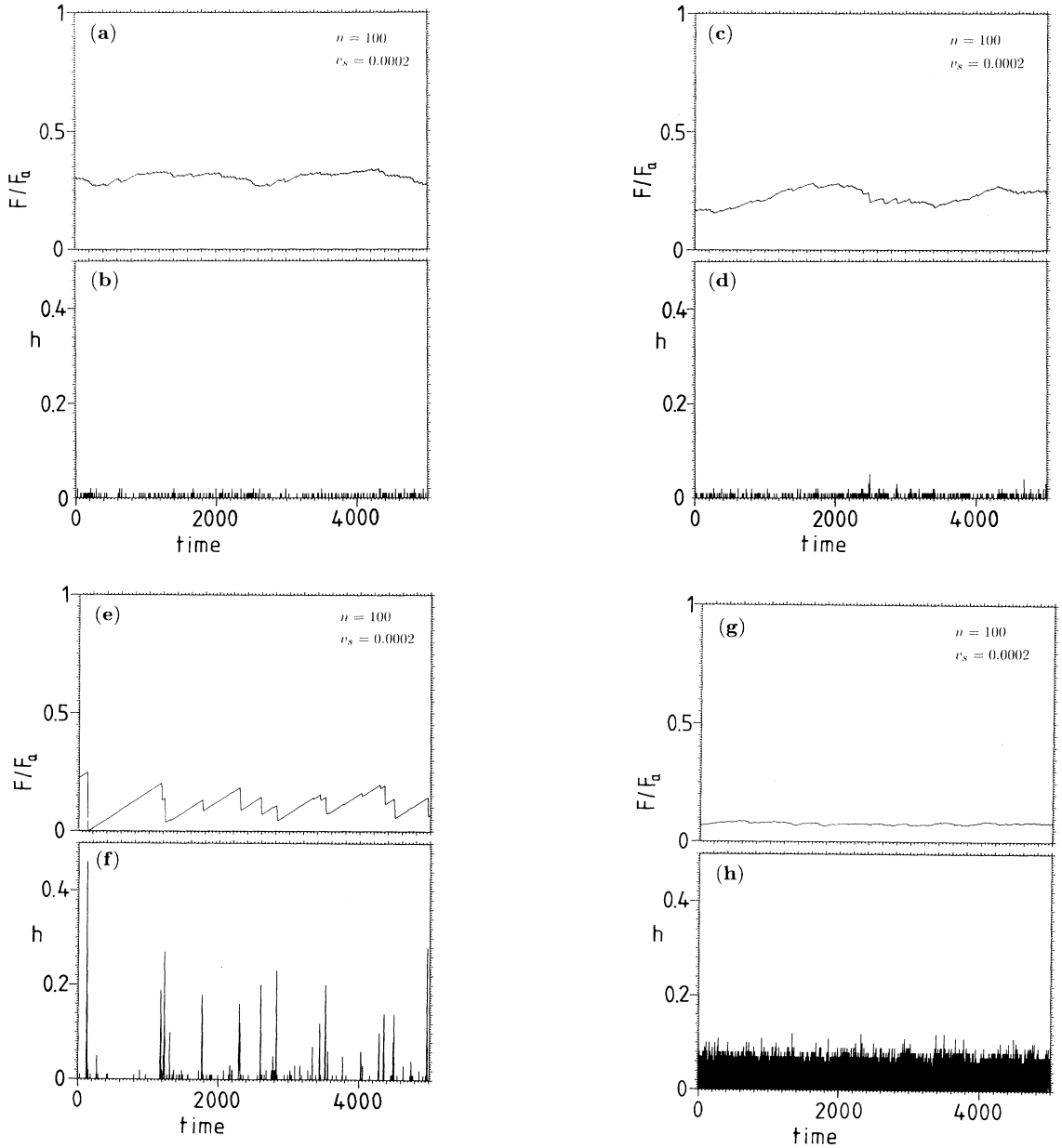

FIG. 13. (a), (c), (e), and (g) show the time variation of the friction force, and (b), (d), (f), and (h) the fraction of moving blocks. (a) and (b) are at zero temperature and (c) and (d) at a finite temperature ($\nu = 0.1$ and $\beta = 40$) and for $k_1 = k_2 = \bar{\gamma} = 1$. (e) and (f) and (g) and (h) are the same as (a) and (b) and (c) and (d), respectively, but now for $k_2 = 50$. In the calculations the number of blocks $n = 100$ and the sliding velocity $v_s = 0.0002$.

separated by other nonsliding blocks. Hence we conclude that only very localized slip events occur in the present model. When thermal processes are included, the same qualitative picture occur; see Figs. 13(c) and 13(d), where $\nu=0.1$ and $\beta=40$.

These results differ from those of Carlson and Langer, who found a wide distribution of the sizes of slip events in their model calculations. However, Carlson and Langer only considered systems where the ratio $k_2/k_1 \gg 1$. In fact, they argued that in the context of earthquakes the limit $k_2/k_1 \to \infty$ is relevant. In Figs. 13(e) and 13(f) I show the time variation of the friction force and of the fraction of moving blocks at zero temperature when $k_1=1$ and $k_2=50$ (all earlier calculations were with $k_2=1$). Note that in this case the sliding force F exhibits stick-and-slip oscillations, and the fraction of moving blocks $h(t)$ shows a very wide distribution of sizes of the slip events. The largest slip event involves about 50% of the blocks, while the smallest involves a single block. These results are similar to those of Carlson and Langer. It is easy to understand why large slip events can occur when $k_2 \gg k_1$. It is clear that if $k_2=\infty$ all blocks must slide together, while in the opposite limit, $k_2=0$, the blocks are completely independent of each other and only slip events involving a single block can occur.

It is interesting to study the influence of thermal processes on the sliding dynamics in Figs. 13(e) and 13(f). In Figs. 13(g) and 13(h) I show the time variation of the friction force and of the fraction of moving blocks at a finite temperature ($\beta=40$ and $\nu=0.1$) but with all other parameters the same as in Figs. 13(e) and 13(f). Note that in this case smooth sliding occurs (i.e., no stick-and-slip oscillations) while about 8% of the blocks move at any time. This is consistent with the general observation[19] that stick-and-slip motion is favored in hard materials such as siliceous rocks, especially those containing quartz, while it is inhibited by the presence of soft, ductile minerals like calcite, serpentine, and clay which may more easily undergo creep motion when exposed to a tangential stress. Similarly, an increase in the temperature may bring about a transition from stick-and-slip motion to smooth sliding. This has been suggested to determine the depth limit of tectonic earthquakes.[19]

E. On the origin of stick-and-slip motion

Stick-and-slip motion can have several different origins.[17] Some are related to inertia effects while other mechanisms are independent of inertia. Here we focus on experiments by Yoshizawa and Israelachvili.[8] They have shown that when sliding a mica crystal on a mica substrate with an intervening lubrication film of molecular thickness, a critical velocity $v_c \sim 1$ μm/s exists such that for spring velocities $v_s > v_c$ smooth sliding occurs, while stick-and-slip motion occurs for $v_s < v_c$.

Let us first note the following. Suppose that the big block slides with the velocity v as the bottom surface of the block suddenly stops moving. As discussed elsewhere,[17] this will generate a stopping wave which propagates with the transverse sound velocity toward the upper surface of the block. Only after the time $\Delta t = d/c$ is the whole block stationary. When the motion of the bottom surface of the block stops, the tangential surface stress increases with $\Delta\sigma = \rho c v$, where ρ is the mass density and c the transverse sound velocity in the block (see Ref. 17). In a typical case $\rho \sim 3000$ kg/m^3, $c \sim 3000$ m/s, and $v_c \sim 1$ μm/s, so that $\Delta\sigma \sim 10$ N/m^2 which is an extremely small increase in the tangential surface stress compared with the magnitude of the shear stress σ itself which is typically equal to $\sigma \sim 10^7$ N/m^2 during sliding. Hence it is likely that thermal or mechanical fluctuations in the system can generate the initial pinning of the surfaces. The fundamental question now is if this initial pinning will survive or if it will immediately be removed as a result of the increase in the spring force with increasing time.

To discuss this question, let us assume that after the return to the pinned state the static friction force depends only on the time of stationary contact τ, $F_0=F_0(\tau)$. We assume that $F_0(0)=F_k$ and that $F_0(\tau)$ increases monotonically with the contact time τ. I will now show that, in order to be consistent with the experimental data of Yoshizawa and Israelachvili, $F_0(\tau)$ must have the general form shown by the solid line in Fig. 14. The dashed lines in Fig. 14 shows the increase in the *spring force*, $k_s v_s \tau$, as a function of the contact time for three different cases (1)–(3). In case (1) the spring force increases faster with τ than the initial linear increase of the static friction force; hence the motion of the block will not stop and no stick and slip motion will occur. If the spring velocity v_s is lower than the critical velocity v_c [cases (2) and (3)] determined by the initial slope of the $F_0(\tau)$ curve [$k_s v_c = dF_0/d\tau$ ($\tau=0$)], the spring force will be smaller than the static friction force $F_0(\tau)$ until τ reaches the values τ_2 [case (2)] or τ_3 [case (3)], at which time slip starts. In these cases stick-and-slip motion will occur. The discussion in this section is a mathematical formulation of an idea already proposed by Yoshizawa and Israelachvili.[8]

There are a number of observations which require $F_0(\tau)$ to have the qualitative form shown in Fig. 14. For example, it has been found that when v_s is reduced from above v_c to below v_c the amplitude ΔF of the stick-and-slip oscillations increases abruptly from zero to a finite

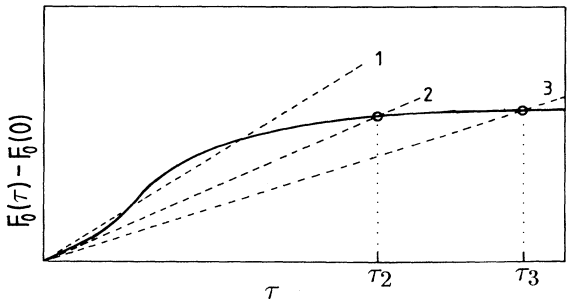

FIG. 14. Solid lines are the variation of the static friction force with stopping time. Dashed lines are the variation of the spring force for three different (1)–(3) sliding velocities, $v_1 > v_c$ but $v_c > v_2 > v_3$.

value, which increases only very slowly as v_s is decreased further toward zero. The fact that ΔF increases abruptly rather than gradually at v_c implies that the $F_0(\tau)$ curve must increase linearly with τ for small τ, followed by an intermediate time period where $F_0(\tau)$ increases faster than linear, and finally an asymptotic time region where $F_0(\tau)$ increases very slowly [e.g., as $F_0 \sim a + b \ln(\tau/\tau_0)$] with increasing τ.

In real systems perpendicular relaxation processes also occur (not accounted for in the model studied in Secs. III B and III C), which may result in stick-and-slip motion in some parts of the (k_s, v_s) kinetic phase diagram. One such mechanism is related to the increase in the contact area with contact time, and will be discussed further below. In the measurements by Yoshizawa and Israelachvili the contact area is kept constant, and there must be a different explanation for the observed stick-and-slip motion. One possibility is the following: At low sliding velocities the lubrication film has a granular state with pinned adsorbate domains. Now, assume that in the sliding state a solid adsorbate domain is pinned by only one of the two solid surfaces as discussed in Sec. III A. When the sliding motion stops, slow rearrangement processes occur in the lubrication layer which finally result in islands being pinned by both of the solid surfaces. This leads to an increase in the static friction force with increasing contact time τ, and $F_0(\tau)$ may take the form indicated in Fig. 14.

Finally, I give some remarks on practical sliding systems where many contact areas (junctions) usually occur between the sliding surfaces. I focus on the friction study of Heslot *et al.*[20] for the sliding of paper on paper. They studied the transition from smooth to stick-and-slip motions, and mapped out a dynamic phase diagram, i.e., the regions in the (k_s, v_s) plane where smooth and stick-and-slip motions occur was determined.

The sliding friction study of Heslot *et al.* differs in a fundamental way from those of Israelachvili *et al.* and Reiter *et al.* In the latter studies a single contact area (junction) occurs where the normal pressure is well below that necessary for plastic or brittle deformation of the block and substrate—the deformations are purely elastic. However, in the study by Heslot *et al.* the normal pressure at a junction is essentially determined by the yield strength of the material. When a block is placed on a substrate, plastic deformation occurs at the contact points, and the local stresses equal the plastic yield stress. Now plastic deformation can be considered as resulting from fluidization and refreezing of small volume elements (cubes); a cube fluidizes when the elastic stresses it is exposed to by the surrounding cubes satisfy some yield criteria (e.g., the von Mises yield condition), and when the cube refreezes the elastic stresses in the cube are strongly reduced. [For metals, the diameter of a cube may be taken to be of the order of the average distance between two nearby dislocations. Fluidization of a cube occurs when the local elastic stresses from the nearby cubes pull the dislocation over its pinning potential barrier, resulting in rapid slip. When the dislocation returns to a pinned state (the freezing transition) the local elastic shear stresses in the cube have a much lower value than before the slip.] This model of plastic deformation is very similar to the model studied in Secs. III B and III C, and one therefore expects that immediately after the rapid plastic deformations which occur when the block is put on the substrate, the cubes in the vicinity of the contact area will be in a critical state with a distribution of local stresses such that some cubes are almost ready to undergo plastic deformation. Just as in the discussion in Sec. III C, this implies that thermal processes will be of crucial importance; slow relaxation (creep) will occur and the contact area will increase slowly with time. Following the discussion in Sec. III C, one can argue that the contact area between the two solids increases with the contact time τ according to the formula

$$\delta A = A_1[1 + g \ln(\tau/\tau_0)] ,$$

as is indeed observed experimentally.[19] This process will influence the kinetic friction force during creep motion since it will take some time $\tau = l/v$ before a contact area is broken, where l is of the order of the diameter of the contact area. Hence during smooth sliding the friction force

$$F = [1 - g \ln(v\tau_0/l)] \left[F_k + \frac{F_0}{4\beta\epsilon} \ln \left[\frac{2\beta\epsilon k_1 v}{F_a \nu} \right] \right]$$

$$\approx \text{const} + \left[\frac{F_0}{4\beta\epsilon} - g F_k \right] \ln v$$

to first order in $\ln(v)$.

F. Experimental implications and discussion

In this section I discuss how the results obtained above may be tested experimentally. In principle there are two different ways to probe experimentally the nature of the lubrication layer during sliding. One way is to use neutron or x-ray scattering to obtain information about the orientation of the lubrication molecules at the interface.[28] Using this method it may be possible to probe whether lubrication molecules during smooth sliding occur in a 2D fluid state or if a granular state occurs with solid domains. Another interesting method would be to study the sound waves generated at the sliding interface. If the lubrication layer during sliding is in a 2D fluid state, then a very wide (in frequency), uniform (in time) distribution of sound waves is emitted from the sliding interface. However, if the lubrication layer has a granular structure, consisting of pinned solid islands, the sound wave emitted from the interface consists of a sequence of wave pulses. The rate of emission of wave pulses from the interface equals the rate of fluidization of pinned islands, which in turn depends on the sliding velocity, assuming smooth sliding. If the individual wave pulses could be studied experimentally, information about the detailed fluidization process of a single island could be gained. Let us estimate how many islands are fluidized per unit time. Assume that the contact area has a radius $R = 5$ μm. If an average pinned island has a diameter $D = 1000$ Å, then $N \sim 10^5$ island would occur at the interface. Now an island will exist for a time τ before the surface stress

reaches the critical value σ_a necessary for fluidization. At the time of fluidization the local elastic displacement of the solids at the island equals $\Delta l \approx D^2\sigma_a/k_1 \approx 1$ Å. Hence we must have $v\tau = \Delta l$ or $\tau \approx 10^{-4}$ s if $v = 1$ μm/s. Hence the rate of wave pulses emitted from the sliding interface will be of order 10^9 per second. The duration of each wave pulse is of the order of $D/c \sim 10^{-11}$ s. These estimates are very rough, but indicate that it may be possible to resolve the individual wave pulses.

IV. SUMMARY AND CONCLUSIONS

During sliding of a block on a lubricated substrate, the friction force at low sliding velocities is usually found to be velocity independent. This indicates that rapid processes occur at the sliding interface, even if the center of mass of the block moves arbitrary slowly relative to the substrate. In this paper I have suggested that, in boundary lubrication, the lubrication layer has a granular state with solid pinned adsorbate islands which fluidize and reform during the sliding process. During the time period that an adsorbate domain remains in a fluidized state, the local elastic stresses built up in the elastic bodies during sticking will be released, partly by emission of elastic wave pulses (sound waves) and partly by shearing the lubrication fluid.

At low sliding velocity stress domains occur in the block and the substrate. In the absence of thermal excitations (i.e., zero temperature), the stress domains form a critical state, with a continuous distribution $P(\sigma)$ of local surface stresses σ extending to the critical stress σ_a, necessary for fluidization of the pinned adsorbate structure. The role of temperature-activated processes (relaxation and creep) has been studied and correlated with experimental observations. In particular, the model explains in a natural manner the logarithmic time dependence observed for various relaxation processes; this time dependence follows from the occurrence of a sharp steplike cutoff at $\sigma = \sigma_a$ in the distribution $P(\sigma)$ of surface stresses. Finally, I have suggested a simple experiment to test directly the theoretical predictions: by registering the elastic wave pulses emitted from the sliding junction, e.g., by a piezoelectric transducer attached to the elastic block, it should be possible to prove whether, during uniform sliding at low velocities, rapid fluidization and refreezing of adsorbate domains occur at the interface.

The theory presented in this paper may have implications for other sliding friction problems, e.g., the sliding of charge-density waves.[29]

APPENDIX A

I estimate the prefactor ν in expression (7) for the probability rate for a stress domain to jump over the barrier to the sliding state. We can visualize this process to occur by a bulk phonon wave packet arriving to the stress block and locally increase the stress to the level necessary for the block to start to slide. Since the motion of a stress block is overdamped, we use Kramers' formula in the overdamped limit to obtain

$$\nu \approx \omega_0^2/(2\pi\gamma) ,$$

where (see Sec. III B) $\omega_0^2 = k_1/m \sim c^2/D^2$ and $\gamma \sim c/D$. Hence

$$\nu \sim c/(2\pi D) .$$

Assuming $c \sim 2000$ m/s and $D \sim 300$ Å gives $\nu \sim 10^{10}$ s^{-1}.

APPENDIX B

Let us first derive an equation of motion for the distribution function $P(\sigma,t)$, which we assume is normalized so that

$$\int_{-\sigma_a}^{\sigma_a} d\sigma\, P(\sigma,t) = 1 . \tag{B1}$$

Let $N(\sigma,t)$ be the number of stress blocks having surface stress between σ and $\sigma+\Delta\sigma$. We have $N(\sigma,t) = N_0 P(\sigma,t)\Delta\sigma$, where N_0 is the total number of stress blocks. Assume that $x = vt$, i.e., that the big block moves with velocity v. Let us consider the short-time interval Δt it takes for the surface stress σ of a pinned block to increase with the amount $\Delta\sigma$, i.e., $k_1 v\Delta t = \delta A\Delta\sigma$. Let us now write down an equation for the number of stress blocks which, at time $t+\Delta t$, have surface stresses between σ and $\sigma+\Delta\sigma$. We have

$$N(\sigma,t+\Delta t) = N(\sigma-\Delta\sigma,t) - N(\sigma,t)\Delta t\nu e^{-\beta\Delta E(\sigma)} + \delta_{\sigma,0}\left[\sum_{\sigma'} N(\sigma',t)\Delta t\nu e^{-\beta\Delta E(\sigma')} + N(\sigma_a,t)\right] .$$

The first term on the right-hand side of this equation describes the number of stress blocks which at time t had the stress in the region $\sigma-\Delta\sigma$ to σ; at time $t+\Delta t$ these stress blocks occur in the stress region σ to $\sigma+\Delta\sigma$ because of the motion $x = vt$. The second term describes the number of stress blocks which have been thermally excited out of the same stress region. Note that $\Delta E(\sigma) = U(\sigma_a) - U(\sigma)$ is the elastic barrier which must be overcome by thermal excitation before the block will be removed from the stress interval σ to $\sigma+\Delta\sigma$. Finally, the last term, which is nonzero only if $\sigma = 0$, describes the increase in the number of stress blocks with zero surface stress which results from all the stress blocks which have been thermally excited over the barrier $\Delta E(\sigma) = U(\sigma_a) - U(\sigma)$ or driven over the barrier by the motion $x(t)$; we assume that after fluidization of the adsorbate layer a block rapidly relaxes down to the state where the surface stress equals zero, after which the adsorbate layer refreezes and the block returns to the pinned state. Now, expanding in the small quantities Δt and $\Delta\sigma$, using $\Delta\sigma/\Delta t = k_1 v/\delta A$, gives

$$\frac{\partial N}{\partial t}+\frac{k_1 v}{\delta A}\frac{\partial N}{\partial \sigma}=-\nu N e^{-\beta\Delta E(\sigma)}+\delta_{\sigma,0}\left[\sum_{\sigma'}\nu N(\sigma',t)e^{-\beta\Delta E(\sigma')}+\frac{N(\sigma_a,t)}{\Delta t}\right].$$

Going to the continuous limit by replacing

$$\delta_{\sigma,0}\sum_{\sigma}\rightarrow\delta(\sigma)\int d\sigma\ ,$$

$$\delta_{\sigma,0}/\Delta t\rightarrow(k_1 v/\delta A)\delta(\sigma)$$

gives

$$\frac{\partial P}{\partial t}+\frac{k_1 v}{\delta A}\frac{\partial P}{\partial \sigma}=-\nu P e^{-\beta\Delta E(\sigma)}+\delta(\sigma)\left[\int d\sigma'\nu P(\sigma',t)e^{-\beta\Delta E(\sigma')}+\frac{k_1 v}{\delta A}P(\sigma_a,t)\right]. \tag{B2}$$

Note that this equation conserves probability: integrating (B2) over σ from $-\sigma_a$ to σ_a, using $P(-\sigma_a,t)=0$ (we assume sliding along the positive-x direction) gives

$$\frac{d}{dt}\int_{-\sigma_a}^{\sigma_a}d\sigma\,P(\sigma,t)=0\ ,$$

so that if the normalization condition (B1) is satisfied at time $t=0$ it will be automatically satisfied for all other times.

Let us study steady sliding. In this case $\partial P/\partial t=0$ and (B2) reduces to an ordinary differential equation for $P(\sigma,t)\equiv P(\sigma)$:

$$\frac{k_1 v}{\delta A}\frac{dP}{d\sigma}=-\nu P e^{-\beta\Delta E(\sigma)}+\delta(\sigma)\left[\int d\sigma' P(\sigma',t)e^{-\beta\Delta E(\sigma')}+\frac{k_1 v}{\delta A}P(\sigma_a,t)\right],$$

with the solution

$$P(\sigma)=C\theta(\sigma)e^{-(\delta A\nu/k_1 v)\int_0^{\sigma}d\sigma'\exp[-\beta\Delta E(\sigma')]}, \tag{B3}$$

where C is determined by the normalization condition (B1). The force F which give rise to the sliding velocity v is determined by the equation

$$F=\frac{\int_{-\sigma_a}^{\sigma_a}d\sigma\ A\sigma P(\sigma)}{\int_{-\sigma_a}^{\sigma_a}d\sigma\,P(\sigma)}\ . \tag{B4}$$

Let us first consider the large-v limit. Assume that $\alpha\ll 1$, where $\alpha=F_a\nu/(2k_1 v\beta\epsilon)$. In this case, to leading order in $\alpha\sim 1/v$, Eq. (B3) gives

$$P(\sigma)\sim C\left[1-\frac{2\alpha\beta\epsilon}{\sigma_a}\int_0^{\sigma}d\sigma' e^{-\beta\Delta E(\sigma')}\right].$$

Substituting this into (B4) gives, to leading order in $1/v$,

$$F=\frac{F_0}{2}\left[1-2\alpha\beta\epsilon\int_0^1 d\xi(\xi-\xi^2)e^{-\beta\Delta E(\xi\sigma_a)}\right], \tag{B5}$$

where $F_0=\sigma_a A$ is the static friction force after an infinitely long contact time. Using $\Delta E=\epsilon[1-(\sigma/\sigma_a)^2]$ the integral in (B5) can be evaluated to give

$$F\sim\frac{F_0}{2}\left[1-\frac{\alpha}{2\beta\epsilon}\right]=\frac{F_0}{2}\left[1-\frac{F_a\nu}{k_1 v}\left[\frac{k_B T}{2\epsilon}\right]^2\right]. \tag{B6}$$

Next let us consider small sliding velocities. Assume that $\alpha\gg 1$ but $\alpha\exp(-2\beta\epsilon)\ll 1$. In this case the sliding force can be evaluated as follows. Let us consider the integral I which occur in the nominator of (B4):

$$I=\int_0^{\sigma_a}d\sigma\,\sigma e^{-(2\alpha\beta\epsilon/\sigma_a)\int_0^{\sigma}d\sigma'\exp\{-\beta\epsilon[1-(\sigma'/\sigma_a)^2]\}}=\sigma_a^2(1/2+J)\ ,$$

where

$$J=\int_0^{\sigma_a}d(\sigma/\sigma_a)(\sigma/\sigma_a)(e^{-(2\alpha\beta\epsilon/\sigma_a)\int_0^{\sigma}d\sigma'\exp\{-\beta\epsilon[1-(\sigma'/\sigma_a)^2]\}}-1)\ .$$

Now it is easy to see that the main contribution to J comes from when $\sigma \approx \sigma_a$ and $\sigma' \approx \sigma_a$. Hence let us introduce

$$\sigma = \sigma_a(1-\xi) ,$$

$$\sigma' = \sigma_a(1-\zeta) ,$$

expand relevant terms to linear order in ξ and ζ, and perform the ξ integral. This gives, after a few simplifications,

$$J = \int_0^1 d\zeta (e^{-\alpha \exp(-2\beta\epsilon\zeta)} - 1) .$$

Let us set $\eta = \exp(-2\beta\epsilon\zeta)$ so that

$$J = \int_{e^{-2\beta\epsilon}}^1 \frac{d\eta}{2\beta\epsilon\eta}(e^{-\alpha\eta} - 1) .$$

Since we have assumed $\alpha \gg 1$ the leading contribution to J for small v will be

$$J \sim -\int_{1/\alpha}^1 \frac{d\eta}{2\beta\epsilon\eta} = -\frac{1}{2\beta\epsilon} \ln(\alpha) .$$

The denominator in (B4) can be evaluated in a manner similar to the nominator, and equals $\sigma_a(1+J)$. Hence, to leading order the sliding friction is given by

$$F = \tfrac{1}{2} A \sigma_a \frac{1+2J}{1+J}$$

$$\sim \frac{F_0}{2}(1+J) = \frac{F_0}{2}\left[1 + \frac{1}{2\beta\epsilon} \ln\left[\frac{2\beta\epsilon k_1 v}{F_a \nu}\right]\right] . \quad \text{(B7)}$$

In the extreme low-v limit, where $\alpha \exp(-2\beta\epsilon) \gg 1$, only the $\sigma \approx 0$ region in the integral in the exponent of (B3) will contribute, and we can approximate

$$P(\sigma) \sim C\theta(\sigma) e^{-(\delta A \nu \sigma / k_1 v) \exp[-\beta\Delta E(0)]} .$$

Substituting this into (B4) gives

$$F \sim (F_0 / 2\alpha\beta\epsilon) e^{\beta\epsilon} = N_0 (k_1 v / \nu) e^{\beta\epsilon} .$$

Note that $F \ll F_0$, and that the friction force is proportional to the sliding velocity v: this is the creep region.

Next let me show how result (12) obtained above by elementary arguments can be obtained from Eq. (B2). Consider the time variation of the stress distribution $P(\sigma t)$ after an abrupt stop of the sliding motion at time $t = 0$, i.e., $v = 0$ for $t > 0$. In this case, for $t > 0$, Eq. (B2) reduces to the ordinary differential equation

$$\frac{dP}{dt} = -\nu P e^{-\beta\Delta E(\sigma)} + \delta(\sigma) \int d\sigma' \nu P(\sigma', t) e^{-\beta\Delta E(\sigma')} .$$

This equation gives

$$P(\sigma, t) = C e^{-\nu t \exp[-\beta\Delta E(\sigma)]} + \delta(\sigma) \int_0^t dt' \nu \int_0^{\sigma_a} d\sigma' C e^{-\nu t' \exp[-\beta\Delta E(\sigma')] - \beta\Delta E(\sigma')} . \quad \text{(B8)}$$

We assume that $\Delta E = \epsilon[1 - (\sigma/\sigma_a)^2]$, and substitute result (B8) into (B4) to obtain

$$F = \int_0^{\sigma_a} d\sigma \; A(\sigma/\sigma_a) e^{-\nu t \exp\{-\beta\epsilon[1-(\sigma/\sigma_a)^2]\}} .$$

Introducing

$$\sigma = \sigma_a(1-\xi) ,$$

$$\eta = e^{-2\beta\epsilon\xi}$$

gives

$$F = \frac{F_0}{\beta 2\epsilon} \int_{e^{-\beta 2\epsilon}}^1 \frac{d\eta}{\eta} \left[1 + \frac{\ln\eta}{\beta 2\epsilon}\right] e^{-\nu t \eta}$$

$$\sim \frac{F_0}{\beta 2\epsilon} \int_{e^{-\beta 2\epsilon}}^{1/\nu t} \frac{d\eta}{\eta} \left[1 + \frac{\ln\eta}{\beta 2\epsilon}\right] .$$

To first order in $1/\beta\epsilon$ this equation gives

$$F \sim F_0 \left[\frac{1}{2} - \frac{\ln \nu t}{\beta 2\epsilon}\right] ,$$

and hence $\Delta F / F_0 \sim (\beta 2\epsilon)^{-1} \ln \nu t$ in agreement with (12).

[1] F. P. Bowden and D. Tabor, *Friction and Lubrication* (Methuen, London, 1967).

[2] E. Rabinowicz, *Friction and Wear of Materials* (Wiley, New York, 1965).

[3] U. Landman, W. D. Luedtke, N. A. Burnham, and R. J. Colton, Science **248**, 454 (1990).

[4] J. B. Sokoloff, J. Appl. Phys. **72**, 1262 (1992).

[5] K. Shinjo and M. Hirano, Surf. Sci. **283**, 473 (1993).

[6] H. Matsukawa and H. Fukuyama, Phys. Rev. **49**, 17 286 (1994).

[7] G. A. Tomlinson, Philos. Mag. **7**, 905 (1929).

[8] H. Yoshizawa and J. Israelachvili, J. Phys. Chem. **97**, 11 300 (1993).

[9] M. L. Gee, P. M. McGuiggan, and J. N. Israelachvili, J. Chem. Phys. **93**, 1895 (1990).

[10] J. N. Israelachvili, Surf. Sci. Rep. **14**, 109 (1992).

[11] S. Granick, Science **253**, 1374 (1991).

[12]G. Reiter, A. L. Demirel, and S. Granick, Science **263**, 1741 (1994); G. Reiter, A. L. Demirel, J. Peanasky, L. Cai, and S. Granick, J. Chem. Phys. **101**, 2606 (1994).

[13]P. A. Thompson and M. O. Robbins, Phys. Rev. A **41**, 6830 (1990); Science **250**, 792 (1990); **253**, 916 (1991); P. A. Thompson, M. O. Robbins, and G. S. Grest, in *Computations for the Nano-Scale,* edited by P. E. Blöchl, C. Joachim, and A. J. Fisher, Vol. 240 of *NATO Advanced Study Institute Series E: Applied Science* (Kluwer, Dordrecht, 1993), p. 127.

[14]B. N. J. Persson, Phys. Rev. Lett. **71**, 1212 (1993).

[15]B. N. J. Persson, Phys. Rev. B **48**, 18 140 (1993).

[16]B. N. J. Persson, in *Computations for the Nano-Scale* (Ref. 13), p. 21.

[17]B. N. J. Persson, Phys. Rev. B **50**, 4771 (1994).

[18]E. Rabinowicz, Proc. Phys. Soc. London **71**, 668 (1958).

[19]*The Mechanics of Earthquakes and Faulting* (Cambridge University Press, Cambridge, 1990).

[20]F. Heslot, T. Baumberger, B. Perrin, B. Caroli, and C. Caroli, Phys. Rev. E **49**, 4973 (1994).

[21]G. Reiter, A. L. Demirel, J. Peanasky, L. Cai, and S. Granick (unpublished).

[22]B. N. J. Persson and E. Tosatti, Phys. Rev. B **50**, 5590 (1994).

[23]I assume that initially a small island is pinned by only one of the two sliding surfaces. This assumption is plausible if the two surfaces are of different materials, giving rise to different pinning potentials, but it may also hold for identical materials, e.g., mica, if (as is always the case in practice) the two lattices are rotated relative to each other.

[24]B. N. J. Persson and R. Ryberg, Phys. Rev. B **32**, 3586 (1985).

[25]L. Knopoff *et al.* [Phys. Rev. B **46**, 7445 (1992)] have presented a simple argument which determine the values of two of the parameters k_1, k_2, and γ. For a free surface (i.e., no frictional coupling) Eq. (1) has wave solutions with the long-wavelength dispersion relation $\omega=-i\gamma/2\pm[(k_2/m)D^2q^2+(k_1/m)-\gamma^2/4]^{1/2}$, where q is the wave vector. Now for a semi-infinite elastic solid one expects the long-wavelength dispersion relation $\omega=cq$, where c is the sound velocity. This will be the case in model (1) only if one sets $\gamma=2(k_1/m)^{1/2}$ and $k_2D^2/m=c^2$. Within a factor of 2 these are the same relations as derived in Sec. III B by other means.

[26]R. Burridge and L. Knopoff, Bull. Seismol. Soc. Am. **57**, 341 (1967).

[27]J. M. Carlson and J. S. Langer, Phys. Rev. Lett. **62**, 2632 (1989).

[28]S. H. J. Idziak, C. R. Safinya, R. S. Hill, K. E. Kraiser, M. Ruths, H. E. Warriner, S. Steinberg, K. S. Liang, and J. N. Israelachvili, Science **264**, 1915 (1994).

[29]See, e.g., G. Grüner, Rev. Mod. Phys. **60**, 1129 (1988).